Dyrk1a Mutations Cause Undergrowth of Cortical Pyramidal Neurons Via Dysregulated Growth Factor Signaling

Jenna A. Levy, Christy W. LaFlamme, George Tsaprailis, Gogce Crynen, Damon T. Page

Supplemental Information

Supplementary Methods and Materials:

Mouse behavior tests

Three-Chamber Social Approach Test: Male mice were tested as previously described (1, 2). Briefly, after at least 2 weeks housing under reversed light cycle, each mouse was habituated in the three-chamber box for 5 min. before a stimulus mouse was placed into a tube in the “social” chamber. The stimulus mice used were young adult male mice. The time spent in each chamber (“mouse + tube”, “empty tube”, “center”) was automatically scored using Ethovision XT software (Noldus).

Marble Burying: Male mice were placed individually in a cage with 5cm of 1/4″ corncob bedding and 20 black marbles (14.3mm in diameter) arranged in a 4 × 5 matrix and left undisturbed for 30 min. The number of marbles that were at least two-thirds buried at the end of the trial were counted.

Tail Suspension Test: Male mice were suspended from a hook with medical tape attached ~2cm from the tail tip for 6 min. The Observer software (Noldus) was used to code and analyze the amount of time that mice were immobile during the trial.

Open Field Test: Male mice were placed individually in the center of the open field arena (43.8 × 43.8 × 32.8cm) under white light with 70dB background white noise for 5 min. Total distance moved, velocity, and time spent in the center versus corners/sides (thigmotaxis) were recorded automatically using Ethovision XT software.

Acoustic Startle and Pre-pulse Inhibition: Each mouse was placed inside a clear acrylic tube (5cm in diameter, 10cm long) secured to a platform with a piezoelectric accelerometer attached beneath the tube (San Diego Instruments) inside a ventilated,

sound-attenuating chamber. Following a 5 min. acclimation period, mice receive trials of white noise stimuli in three phases: I) baseline startle, II) mixed startle and pre-pulse inhibition, and III) final startle. During the test, trials are presented at variable 8-23s inter-trial intervals, and 70dB background white noise is present throughout. Phases I and III consist of 6 startle trials with a white noise stimulus of 40ms at 120dB. During phase II, mice receive a total of 52 trials of three types, presented in a pseudorandom order: i) 12 startle trials (as in phases I and III), ii) 10 control trials (no stimulus), iii) pre-pulse inhibition trials (20ms pre-pulse stimulus at 4, 8, or 16dB above background, followed by 120dB startle stimulus 100ms after pre-pulse onset), 10 for each pre-pulse stimulus. The maximum whole-body flinch response to each startle pulse (whether preceded by a pre-pulse or not) are recorded using SR-Lab software (San Diego Instruments), which takes 65 consecutive 1ms readings from the beginning of stimulus onset. Response to each type of stimulus was averaged across presentations within each phase. Percent pre-pulse inhibition was calculated as [(phase II startle trial – pre-pulse trial) / (phase II startle trial) x 100].

(1-3)IGF-1 treatment: (1-3)IGF-1 was acquired from VWR/Bachem (catalog #H-2468.1000) and dissolved in saline with .01% BSA fresh every day. Intraperitoneal injections of 10µg/g (1-3)IGF-1 or vehicle were delivered daily at 8 a.m. starting on P1 and ending on P7. This dosage was chosen based on multiple studies of (1-3) IGF-1 treatment in ASD mouse models that showed brain penetrance and increased signaling downstream of IGF-1 within 3 hours post-injection (3, 4). Pups were individually removed, injected, and placed back in the home cage with the dam. On P7, 6 hours post-injection, pups were rapidly decapitated for downstream analysis.

Isotropic Fractionator: Isotropic fractionator was used as previously described (5). Briefly, adult animals were perfused with 4% PFA, and pups underwent rapid decapitation and dissection. Brains were fixed in 4% PFA for one week, and then the cortex was dissected out and dissociated in a 7mL glass tissue homogenizer (Kontes Glass) in dissociation buffer (1% Triton X-100 in 40mM sodium citrate). 1mL of nuclei was removed and stained with 1:50 DAPI (Invitrogen, catalog #D3571) before being loaded onto a hemocytometer (Fisher Scientific, catalog #0267110). Per animal, 6 technical replicates of 10µL nuclei were imaged and counted in the hemocytometer (0.1µL nuclei counted per technical replicate). After calculating the total cell number per cortex, the number of cells was divided by mg of cortex to obtain density.

Flow cytometry: After isotropic fractionator, nuclei were stained with DAPI (1:100) and primary (anti-NeuN antibody (1:500; 104225, Abcam)) and secondary (Goat anti-Mouse 488 (1:2000, A21121, Life Technologies)) antibodies, then filtered through a 30µm diameter cell strainer (#352235, Falcon) before analysis. On a Gallios flow cytometer analyzer (Beckman Coulter), DAPI fluorescence was collected with a 450/50 filter (405nm laser) and Alexa 488 with a 550 SP filter (488nm laser). Background fluorescence was determined using a control with only the secondary antibody. The Neu-N+ population was determined by gating the population of single, DAPI+ events above background using FlowJo software. Total neuronal and non-neuronal numbers were calculated by taking the percentage (as determined by flow cytometry) of the total cortical cell number from the same biological sample.

Immunohistochemistry: Adult animals were perfused with 4% PFA, and pups underwent rapid decapitation and dissection. After 18 hours post-fixation in 4% PFA, brains were incubated in a 20% sucrose/PBS solution at 4°C for 2-3 days and embedded in Tissue-Tek OCT compound (Sakura). 40µm sections were collected on Superfrost/Plus slides and stained. The following primary antibodies were used following antigen retrieval (10 min. in boiling 10X citrate buffer): anti-cleaved caspase 3 (1:1000, Cell Signaling Technology, catalog #9661S), anti-Ctip2 (1:2000, Abcam, catalog #18465), anti-p-S6 Ser235/236 (1:2000, Cell Signaling Technology, catalog #4858S). AlexaFluor-488, -594, and -647-conjugated secondary antibodies (1:2000) were purchased from Invitrogen. DAPI was used for nuclear labeling (Invitrogen, catalog #D3571). Slides were mounted with Vectashield HardSet and images were obtained with an Olympus VS120 microscope and processed using the VS-DESKTOP software (Olympus) or ImageJ (NIH).

For morphological measurements (cortical thickness), fixed lines were drawn horizontally at the bottom of a coronal section and a perpendicular vertical line through the midline. Lines at varying degrees were then drawn from the bottom landmark, and cortical thickness was measured at each measurement angle, agnostic of the shape or size of the brain section. This was conducted across 2-3 plane-matched sections per animal. Ventricle size was analyzed by drawing a region of interest (ROI) around the entire ventricle in 2-3 plane-matched sections per animal.

For analysis of laminar marker counts and density, ROIs were cropped in the somatosensory cortex and normalized for width, with the height of the ROI beginning at the top of the ventricle and ending at the pial surface. In ImageJ, the ROI was divided into 10 equal bins. Ctip2+ neurons were counted in each bin using the Cell Counter tool in

ImageJ, then DAPI+ cells were counted in each bin. The density of putative layer V neurons was measured by dividing Ctip2+ neurons by DAPI+ cells per bin.

To measure apoptosis in the cortex, P0 and P4 sections were stained with cleaved caspase 3 (CC3). One whole cortical hemisphere was defined as an ROI; and for each animal, counts of cells positive for CC3 were obtained from 3 plane-matched sections per animal.

For p-S6 intensity, P0, P7, and adult sections were stained with Ctip2 and p-S6 (Ser235/236). This specific antibody has been shown to detect p-S6 *in vivo* in mice (6, 7). After image acquisition, Ctip2+ neurons were measured for p-S6 mean gray intensity. 25-30 neurons were measured per section and 2 plane-matched sections were analyzed per animal.

For soma size analysis, sections were stained with NeuroTrace green fluorescent Nissl stain (1:100 dilution, Life Technologies catalog #N-21480) and washed with PBS. After image acquisition, somas in each layer in somatosensory cortex (S1) were measured using the ImageJ freehand tool. Layers were denoted based on anatomical boundaries using DAPI staining. 30-35 somas were measured per layer and 2-3 plane-matched sections were analyzed per animal. This was done based on a previously published technique (8).

Anterograde tracing: rAAV2-Ef1a-DIO-ChR2 (H134R)-EYFP was obtained from University of North Carolina Vector Core. For injections, mice were anaesthetized under isoflurane and placed onto a stereotaxic frame. Bregma and lambda were used to find the coordinates of the mPFC (1.8mm anterior to bregma, 0.3mm lateral to midline and

2.2mm ventral to bregma). The virus was injected by a syringe pump at a rate of 50nL min^{-1}, with 100nL volume injected per site in each mouse. Mice were perfused 2 weeks later, allowing for the expression of EYFP. 50µm-thick coronal brain sections were collected to image mPFC and axon terminals. For analysis, images were acquired, and fibers were reconstructed using the Simple Neurite Tracer plugin on ImageJ. Number of reconstructed fibers was measured relative to the 80μm^2 ROI.

TMT labelling, phosphopeptide enrichment and quantitative mass spectrometry-based proteomics: Cortices were isolated from P0 control (N=6) and cKO pups (N=7) and dissociated using a dounce homogenizer in 1X lysis buffer (Cell Signaling Technologies). Protein was determined using the BCA protein assay (9) from Pierce as per the manufacturer's instructions. Two 100µg aliquots (total 200µg protein per sample) were dried under vacuum and processed for digestion using two independent micro S-Traps™ (Protifi, Huntington, NY) according to the manufacturer's instructions. Briefly, the dried protein was resuspended in 22µL of 5% SDS, reduced using DTT at 55°C for 10 min., alkylated using methyl methanethiosulfonate (MMTS) at room temperature for 10 min. and then spun down at 20K for 10 min. Subsequently, 2.5µL of phosphoric acid was added to the sample, followed by 165µL of a mixture of HPLC grade methanol and Protifi binding/wash buffer. Following loading onto the S-Trap™, samples were washed three times using centrifugation and trypsin was added in 50mM TEAB at a 1:25 w/w ratio. The S-Trap™ column was incubated for 1 hour at 47°C. Following this incubation, 40µL of 50mM triethylammonium bicarbonate (TEAB) was added to the S-Trap™ and the peptides were eluted using centrifugation. Elution was repeated once. A third elution using 35µL of 50% acetonitrile (ACN) was also performed and the eluted peptides were

dried under vacuum. Peptides were reconstituted in 50mM TEAB, and their concentrations were determined using the Pierce™ quantitative fluorometric peptide assay (Thermo Fisher Scientific, Waltham, MA). Seventy micrograms of peptides were labelled with TMT labels (10-plex) according to the manufacturer's instructions (Thermo Fisher Scientific, Waltham, MA) and pooled. The pooled plexed samples (630 or 700µg total) were dried under vacuum, resolubilized in 1% TFA, desalted using OASIS HLB 1cc solid phase extraction cartridges (Waters, Milldford, MA) and then dried once again using vacuum. TMT-labeled phosphopeptides for mass spectrometry were enriched using the High- Select™ Fe-NTA Phosphopeptide Enrichment Kit from Thermo Fisher Scientific according to the manufacturer's instructions. The TMT-labelled non-phosphopeptide complement was cleaned up for mass spectrometry using a C18 ZipTip according to the manufacturer's instructions (Millipore, Billerica, MA). For mass spectrometry, dried TMT-labelled peptides (phosphopeptides and non-phosphopeptides) were reconstituted in 5µL of 0.1% formic acid, and mass spectrometry was performed as described previously with the exception that separation was performed on as EASY PepMapTM RSLC C18 column (2µm, 100 Å, 75µm x 50cm, Thermo Scientific, San Jose, CA). Ions were created with an EASY Spray source (Thermo Scientific, San Jose, CA) held at 50° C using a voltage of 1.9 kV (10).

Proteomic data processing and statistical analysis: Quantitative analysis of the TMT experiments was performed simultaneously to protein identification using Proteome Discoverer 2.3 software. The precursor and fragment ion mass tolerances were set to 10ppm, 0.6Da, respectively), enzyme was Trypsin with a maximum of 2 missed cleavages and Uniprot Mouse proteome FASTA file was used in SEQUEST searches. The impurity

correction factors obtained from Thermo Fisher Scientific for each kit was included in the search and quantification. The following settings were used to search the phospho-enriched data; dynamic modifications; Oxidation / +15.995Da (M), Deamidated / +0.984Da (N, Q), Phospho / +79.966Da (S, T, Y) and static modifications of TMT6plex / +229.163Da (N-Terminus, K), MMTS +45.987 (C). Only unique+ Razor peptides were considered for quantification purposes. Percolator feature of Proteome Discoverer 2.3 was used to set a false discovery rate (FDR) of 0.01. IMP-ptmRS node was used to calculate probability values for each putative phosphorylation site (11). Only phosphopeptides with a probability value > 75% were included. Total Peptide Abundance normalization method was used to adjust for loading bias and Protein Abundance Based method was used to calculate the protein level ratios. Co-isolation threshold and SPS Mass Matches threshold were set to 50 and 65, respectively. The non-enriched dataset was analyzed in the same fashion except for omission phosphorylation in SEQUEST search and IMP-ptmRS node in PD workflow. Individual proteins were used to compare treatment groups to controls using ANOVA option in Proteome Discoverer and both *P* values and adjusted *P* values were generated.

For predicted upstream analysis, IPA Ingenuity Upstream Regulator was used to identify predicted upstream transcriptional regulators that may account for the altered protein expression in the given dataset. This was measured using an overlap *P* value and an activation z-score based on the altered proteins and phospho-proteins. GO terms were generated using geneontology.org, and the dot plot was generated using a previously described R script (12).

Western blot analysis: Following rapid decapitation, cortices were dissected and homogenized in cell lysis buffer (CST) containing the Protease Inhibitor Cocktail (Roche) and phosphatase inhibitors (Sigma-Aldrich) using a dounce homogenizer. Total protein concentrations were measured using the Pierce BCA Protein Assay Kit (ThermoScientific). 50µg of lysate was loaded and electrophoresed onto NuPAGE 4–12% Bis-Tris Gel (Novex, Life Technologies) and transferred to polyvinylidene difluoride membranes (Immobilon, Millipore). Primary antibodies used in this study, all at 1:2000, were phospho-S6 (p-S6; S235/236; Cell Signaling Technology, #4858), S6 (Cell Signaling Technology, #2217), Erk1/2 (P44/42 MAPK, Cell Signaling Technology, #4695P), p-Erk1/2 (Phospho-P44/42 MAPK, Cell Signaling Technology, #9101), p-S6K (Cell Signaling Technology, #9234S), S6K (Cell Signaling Technology, #2708P), mTOR (Cell Signaling Technology, #2983S), p-mTOR (Cell Signaling Technology, #5536S), p-TrkB (Y816; Millipore, #ABN1381), TrkB (Cell Signaling Technology, #4603), p-Cdc2 (Y15; Cell Signaling Technology, #9111S), Cdc2 (Cell Signaling Technology, #77055), Map2 (Millipore, #AB5622), Tau46 (Cell Signaling Technology, #4019S), and β-actin (Cell Signaling Technology, #4970). Peroxidase-conjugated anti-rabbit or mouse IgG secondary antibody (1:5000, Jackson ImmunoResearch Laboratories, Inc.) was used. Proteins were then visualized after addition of WesternBright Quantum kit (Advansta), imaged using chemiluminescence, and quantified using ImageJ software. Quantification was performed by using the blot tool to measure relative abundance. Phosphorylated proteins were normalized to their total protein abundance (i.e., p-mTOR divided by mTOR).

***In vitro* primary neuronal culture:** Brains from P0 mice were removed, and whole cortices were dissected. Individual cortices were placed into 1mL chilled dissecting media (1X HBSS (14175-095), 30mM glucose, 60µM HEPES). After aspiration of the dissecting media, the tissue was enzymatically dissociated with papain (LS003126) that was previously diluted 1:80 in pre-warmed plating media [Neurobasal A (10888-022), 5% FBS (16000044), and 1% penicillin/streptomycin (p/s) / 0.25% glutamine (10378-016)] and incubated at 37°C for 15 min. The papain was removed, and the tissue was pipetted into a single-cell suspension in plating media. The suspensions were filtered using 40µm nylon cell strainers (Fisher Scientific, #352340), and the filtered suspension was centrifuged at 280 RCF for 5 min. The supernatant was aspirated, and the pellet was re-suspended in pre-warmed plating media. Samples of the suspensions were diluted 1:4 in trypan blue, and cells were counted with a manual hemocytometer for determination of sample concentration. The cells were then plated at 50,000 cells per well in sterile 12-well plates (#07-200-82) containing Poly-D-Lysine (PDL) coated coverslips (GG-18-pdl). On the first day-in-vitro (DIV0), the plating medium was fully exchanged with 1mL feeding medium [Neurobasal A, 1% penicillin / streptomycin / 0.25% glutamine, 2% B-27™ serum-free supplement (17504-044)]. At DIV3, the volume of feeding media was doubled by adding 1mL of feeding medium to all wells, and every three DIV, 1mL of media was replaced with 1mL fresh feeding media until DIV15. Cells were washed with 1X PBS and fixed at DIV15 with 4% paraformaldehyde (PFA) in 1X PBS for 10 min. at room temperature. After undergoing three additional washes in 1X PBS to remove remaining PFA, cells were stored in PBS at 4°C until further use.

For (1-3)IGF-1 treatment, neurons were dosed with either Milli-Q water as vehicle or 100ng/mL of (1-3)IGF-1 (Art. No. 40261041000; CAS No. 32302-76-4) dissolved in Milli-Q water as drug, both sterilized with the Steriflip® Vacuum Driven Filtration System. Dosage was based on previous studies (13). Cells were dosed by removing 1mL feeding media and adding 1mL of vehicle or drug diluted in feeding media for three consecutive days with 24-hour incubation periods in between each dose and a 12-hour incubation period between the final dose and fixation of the cells at DIV15.

For immunocytochemistry, cells were incubated with primary antibodies overnight at 4°C in a humidity chamber. Primary antibodies used include Tuj1 (1:750, Abcam #ab78078) and Ctip2 (1:1000, Abcam #ab18465). The secondary antibodies were diluted in PBS blocking solution and incubated with cells for 1 hour at room temperature. After washing off remaining antibody with 1X PBS, the coverslips were removed from the wells and allowed to dry for 5 min. before being mounted onto slides (48311-703) with Vectashield mounting medium containing DAPI (Life Technologies #P36935).

All coverslip images were taken at 40X magnification on an Olympus VS-120 epifluorescence microscope and analyzed with ImageJ (NIH). The Simple Neurite Tracer plugin was used to draw neurite traces for individual neurons. The Sholl analysis plugin was used to run Sholl analysis on the reconstructed neurite traces after thresholding the images to a binary format.

Statistical Analysis: Power analysis was used to determine sample size using the control mean determined from preliminary data with an alpha of 0.05 and a power of 80%. Planned comparisons between WT and mutant mice were performed for all assays using independent-sample *t* tests. One-way analyses of variance (ANOVAs) were used to

assess genotype effect in experiments containing control, cHet, and cKO or control, cHet, and dHet mice with Tukey's or Sidak's *post hoc* tests used where appropriate. All statistics were performed using GraphPad Prism, with significance set at $P<0.05$. Throughout the manuscript, values represent means; error bars indicate SEMs; N values refer to biological replicates. All measurements and testing were performed blind to the genotype and/or experimental manipulations.

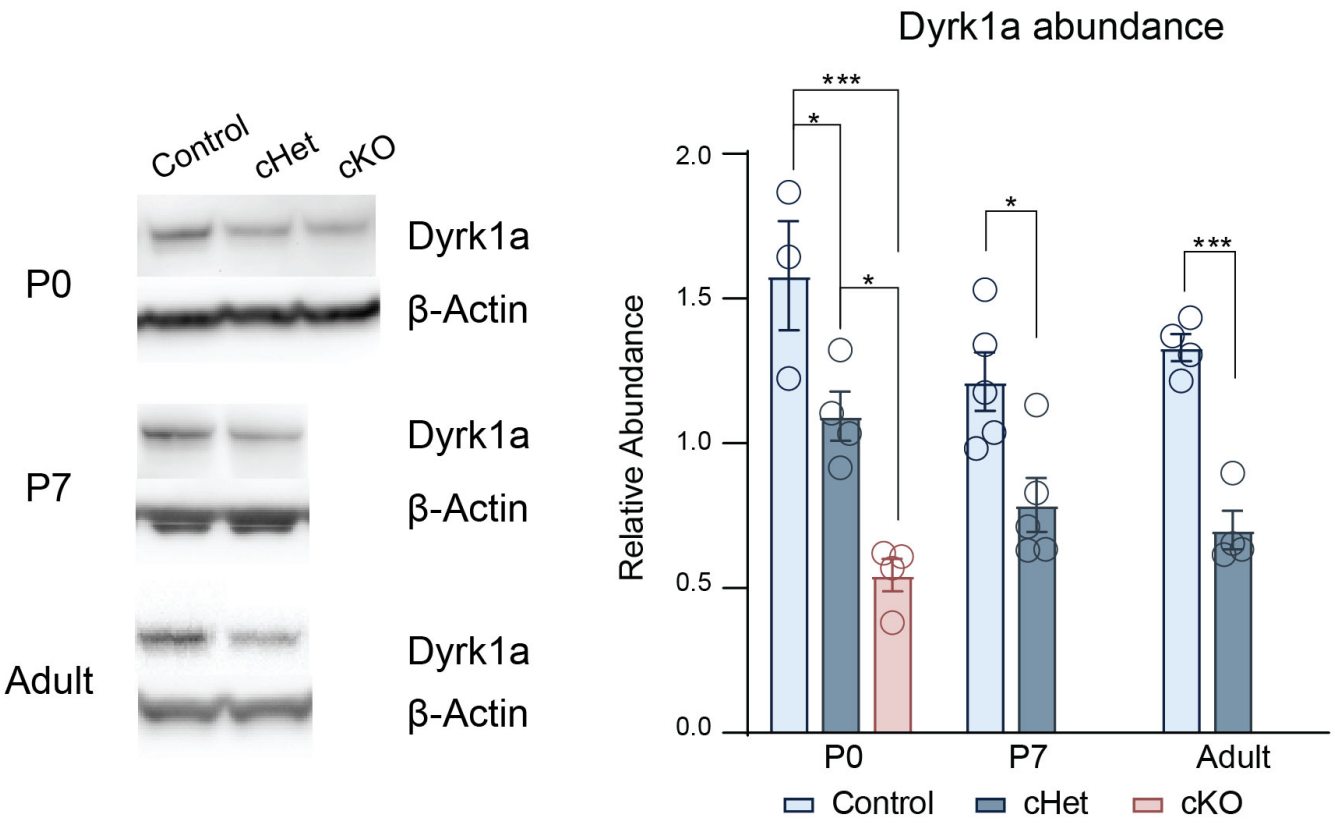

Supplemental Figure S1: Expression of Dyrk1a in the mutant cortex over time and analysis of cortical thickness.

Western blot of cortical lysate from P0 pups with quantification measured as relative abundance in ImageJ. Dyrk1a was normalized to β-Actin. P0 analyzed by one-way ANOVA with Tukey's *post hoc* multiple comparisons tests ($F_{2,8}$=22.01, P=.0006). P7 and adult measured by independent sample *t*-tests (P7: t_8=3.099, P=.014,Adult: t_6=7.782, P=.0002). N=3-5/genotype.

Results from *post hoc* and *t*-tests indicated on graphs. Error bars represent mean +/- SEM. *P<.05, **P<.01, ***P<.001, ****P<.0001.

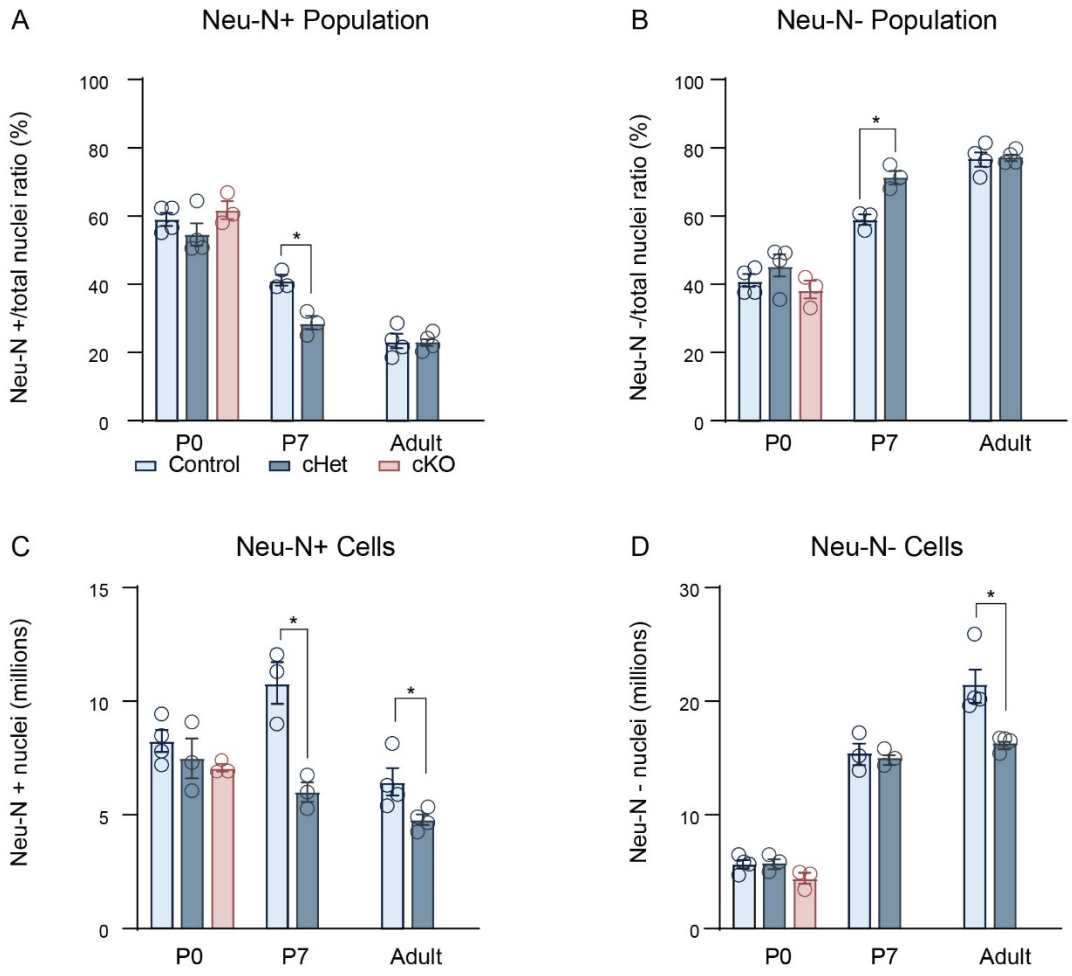

Supplemental Figure S2: Alterations in neuronal and non-neuronal populations drive postnatal microcephaly in cHets.

(A) The proportion of Neu-N+ nuclei is unchanged at P0 and adult but decreased at P7. P0 analyzed by one-way ANOVA $F_{2,8}$=1.704, P=.2419. P7 and adults measured by independent sample *t*-tests (P7: t_4=4.866, P=.008, Adult: t_6=2.323, P=.84).

(B) The proportion of Neu-N- nuclei is unchanged at P0 and adult but increased at P7. P0 analyzed by one-way ANOVA $F_{2,8}$=1.704, P=.2419. P7 and adults measured by independent sample *t*-tests (P7: t_4=4.866, P=.008, Adult: t_6=2.323, P=.84).

(C) The total number of neuronal nuclei is unchanged at P0 but decreased at P7 and adult. P0 analyzed by one-way ANOVA $F_{2,7}$=1.162, P=.3667. P7 and adults measured by independent sample *t*-tests (P7: t_4=4.718, P=.009, Adult: t_6=2.577, P=.042).

(D) The total number of non-neuronal nuclei is unchanged at P0 and P7 but decreased in adults. P0 analyzed by one-way ANOVA $F_{2,7}$=3.148, P=.1059. P7 and adults measured by independent sample *t*-tests (P7: t_4=.37, P=.73, Adult: t_6=3.408, P=.014).

N=3-4/genotype.

Results from *post hoc* and *t*-tests indicated on graphs. Error bars represent mean +/- SEM. *P<.05, **P<.01, ***P<.001, ****P<.0001.

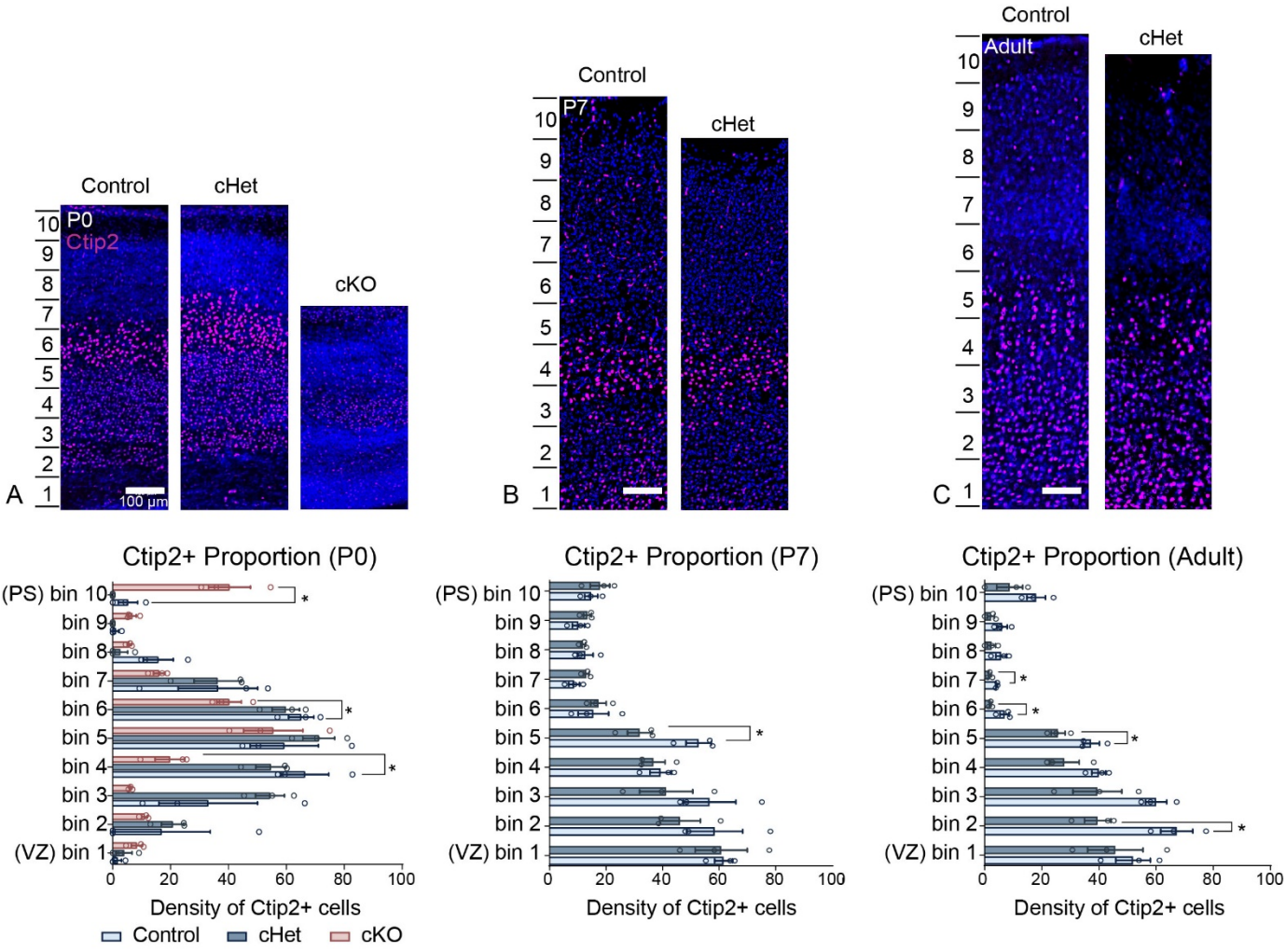

Supplemental Figure S3: Conditional *Dyrk1a* mutants exhibit decreased proportion of layer V neurons.

(A) Representative image of the cortical column in somatosensory cortex of P0 mice stained with Ctip2. Quantification shows there are no alterations in Ctip2+ proportions in cHets. In cKOs, there is a significant decrease in bins related to the approximate layer V location and an increase in the uppermost bin closest to the pial surface (PS) and no alterations near the ventricular zone (VZ). Repeated measure two-way ANOVA with

Tukey's *post hoc* multiple comparisons tests show a significant interaction between bin and genotype ($F_{18,54}$=4.541, P<.0001).

(B) At P7, there is a significant decrease in the Ctip2+ proportion in the bin corresponding to layer V. Repeated measure two-way ANOVA with Sidak's *post hoc* multiple comparisons tests show a significant interaction between bin and genotype ($F_{9,18}$ =3.264 P=.0156).

(C) In adulthood, there is a significant decrease in the Ctip2+ proportion in the bins corresponding to layer V and VI. Repeated measure two-way ANOVA with Sidak's *post hoc* multiple comparisons tests show a significant interaction between bin and genotype ($F_{9,36}$ =2.412, P=.0294). For all ages, N=3/genotype.

Results from *post hoc* and *t*-tests indicated on graphs. Error bars represent mean +/- SEM. *P<.05, **P<.01, ***P<.001, ****P<.0001.

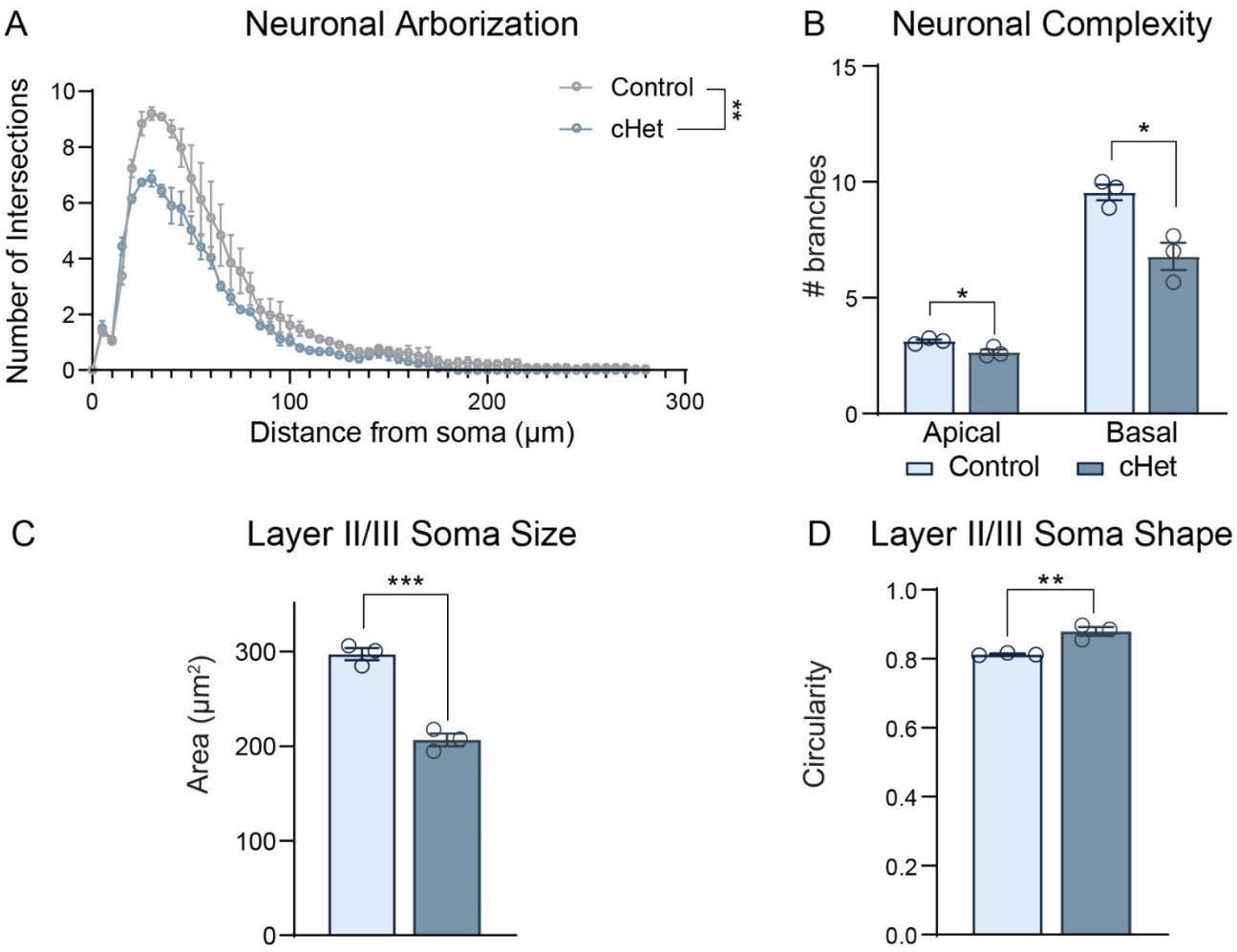

Supplemental Figure S4: *Dyrk1a* cHets exhibit decreased complexity of layer II/III neurons.

(A) Sholl analysis of neuronal arborization on individual layer II/III pyramidal neurons shows that cHets exhibit significantly decreased neuronal arborization (independent sample *t*-test of area under the curve generated for each genotype: t_4=7.234, P=.0019). N=10-15 neurons/mouse, 3 mice/genotype across 2 sections.

(B) cHet layer II/III pyramidal neurons contain less complex basal branches, measured by counting the endpoints on the reconstructed neurons (Apical: t_4=3.378, P=.027848,

Basal: t_4=4.066, P=.015269). (C) Adult cHets putative pyramidal neurons exhibit decreased cell soma size in layer II/III pyramidal neurons in the mPFC (t_4=9.835, P=.0006).

(D) cHet layer II/III pyramidal neurons exhibit more circular somas measured by the circularity plugin in ImageJ (t_4=5.282, P=.0062). N=3/genotype. Results analyzed by independent sample *t*-tests unless otherwise specified.

Results from *post hoc* and *t*-tests indicated on graphs. Error bars represent mean +/- SEM. *P<.05, **P<.01, ***P<.001, ****P<.0001.

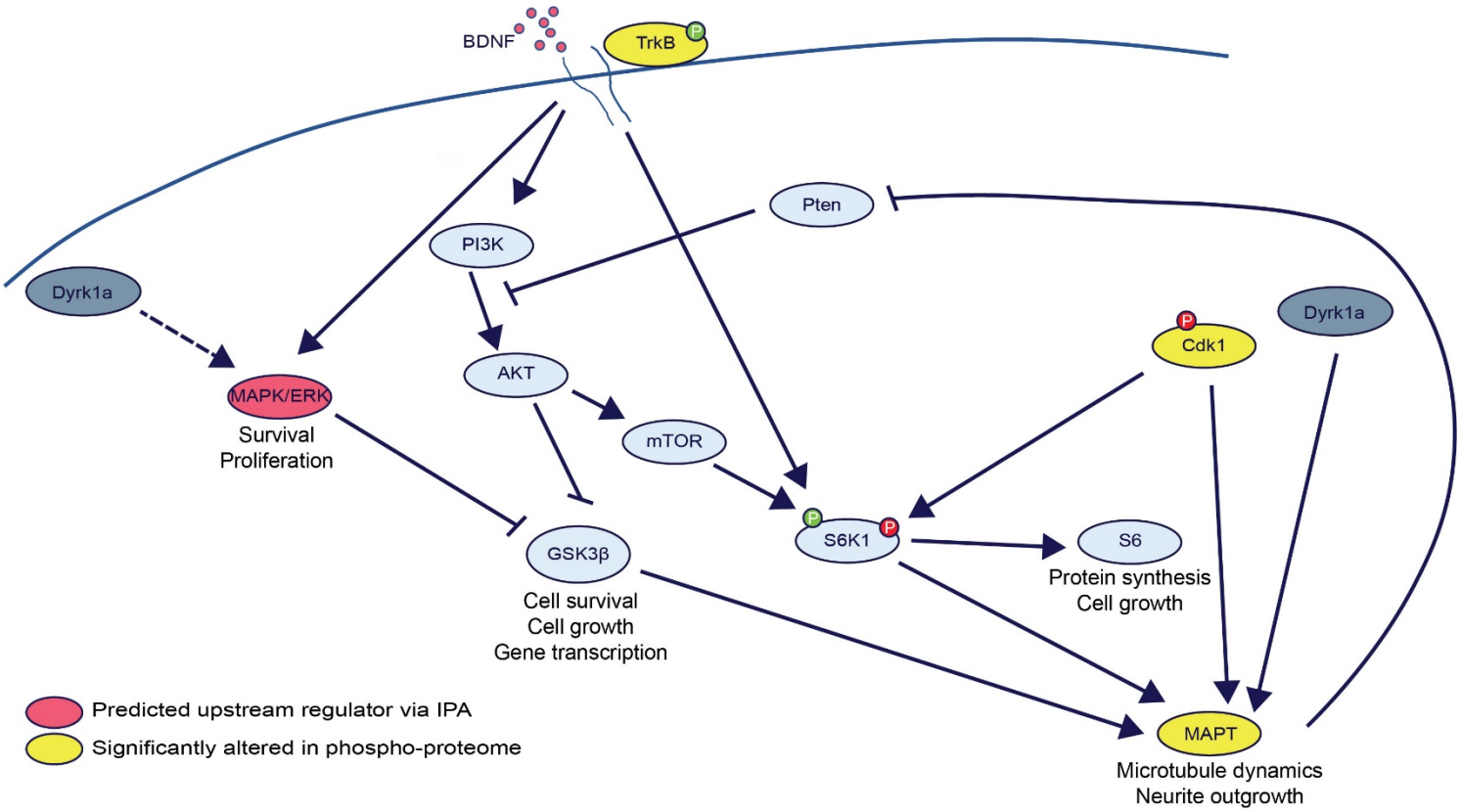

Supplemental Figure S5: Proposed pathway.

A schema of a proposed signaling mechanism by which mTOR and TrkB signaling are regulated in *Dyrk1a* mutants. Decreased *Dyrk1a* dosage causes increased inhibition of GSK3β, which alone is sufficient to cause decreased proliferation and growth, but additionally causes decreased phosphorylation of its target MAPT. MAPT is known to be phosphorylated by Dyrk1a at S202 and S404 (14); however, the phosphopeptide identified by the proteomic experiment is S704. MAPT is a critical regulator of microtubule dynamics and is a negative regulator of Pten. Decreased activation of MAPT would, in turn, cause increased activation of Pten and thus decreased mTOR activity, causing microcephaly and the observed decreased neuronal growth. Cdk1 targets MAPT (15) and

TSC2 (16) (a negative regulator of mTOR). The inhibitory phosphorylation of Cdk1 (Y15) is increased in *Dyrk1a* cKOs, which would theoretically lead to decreased phosphorylation of MAPT and decreased inhibition of TSC2, resulting in decreased mTOR signaling. This was validated using western blot, as p-CDK1 (Y15) was found to be increased relative to total CDK1. Dyrk1a is known to phosphorylate Tau (14) and this phosphorylation site is decreased in the phospho-proteome. MAPT is a negative regulator of Pten (17) and thus is an interesting link between *Dyrk1a* and Pten/mTOR signaling.

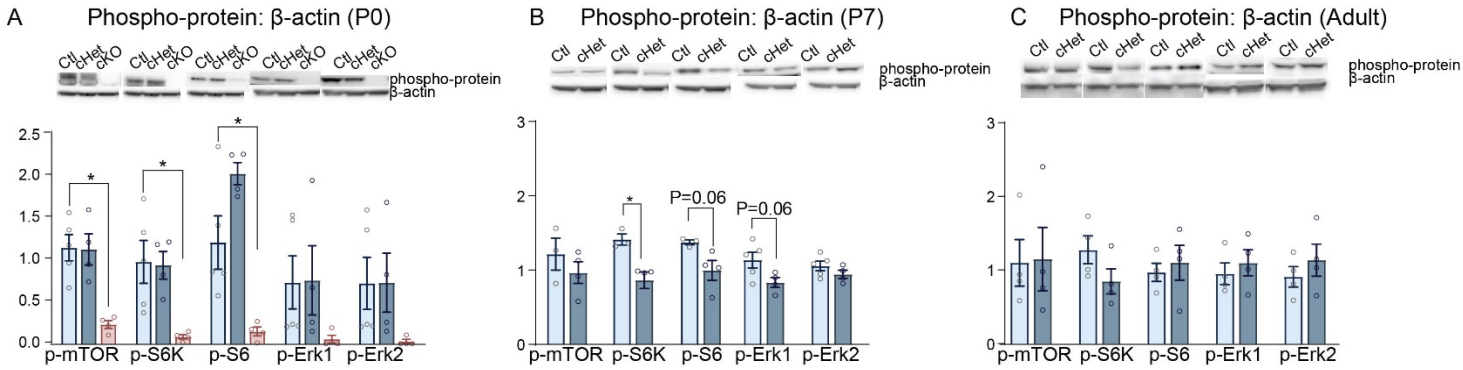

Supplemental Figure S6: Activation of the mTOR pathway is decreased in the cortex of conditional *Dyrk1a* mutants.

(A) P0 cKO cortices exhibit decreased activation of mTOR signaling molecules. Western blot on cortical lysate normalized to β-Actin from P0 pups analyzed by one-way ANOVA with Tukey's *post hoc* multiple comparisons tests (p-mTOR: $F_{2,10}$=12.35, P=.002; p-S6K: $F_{2,10}$=6.5, P=.0155; p-S6: $F_{2,10}$=15.82, P=.0008).

(B) P7 cHets exhibit decreased activation of S6K in the cortex (t_5=3.76018, P=.0132) and a trend towards decreased activation of S6 (t_5=2.38094, P=.063) and ERK1 (t_7=2.21842, P=.062). Analyzed by independent sample *t*-tests.

(C) Adult cHets do not exhibit decreased activation of mTOR relative to a housekeeping gene in the cortex. Analyzed by independent sample *t*-tests. Quantified using relative abundance in ImageJ. For all ages, N=3-5/genotype. Results from *t*-tests indicated on graphs . Error bars represent mean +/- SEM. *P<.05, **P<.01, ***P<.001, ****P<.0001.

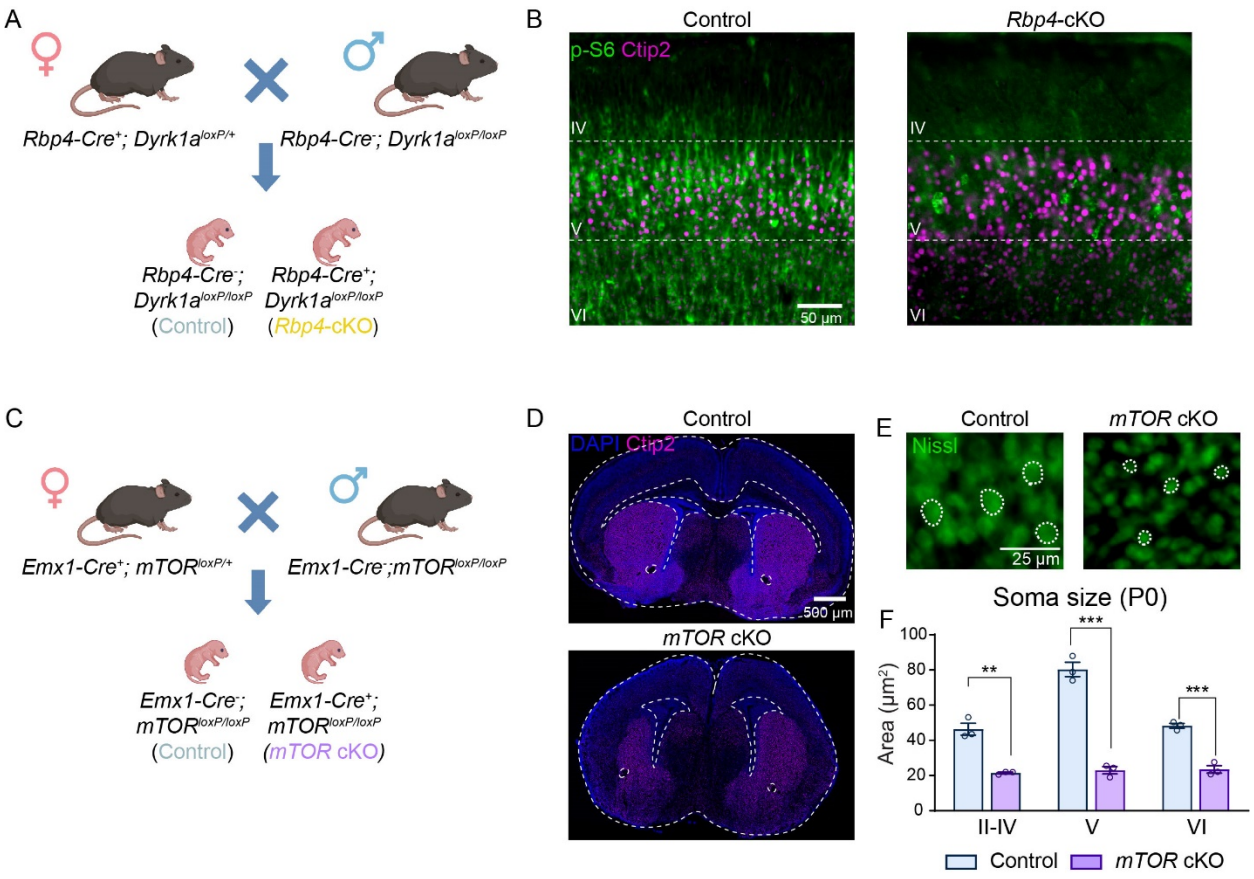

Supplemental Figure S7: Deletion of *Dyrk1a* in layer V neurons is sufficient to drive a reduction in mTOR activation.

(A) Breeding scheme used to generate layer V knockouts of *Dyrk1a*.

(B) Images of the mouse cerebral cortex showing the *Rbp4*-cKO cortex (right) lacks enriched p-S6 staining (green) in layer V neurons (magenta).

(C) Breeding scheme used to generate cortical *mTOR* knockouts.

(D) Images of coronal brain section at birth from control (top) and *mTOR* cKO (bottom) showing that mTOR cKO exhibits a thin/absent corpus callosum, thin cerebral cortex, and abnormally shaped ventricles.

(E) Representative image of Nissl-stained somas in P0 control and *mTOR* cKO cortices.

(F) Quantification of soma size in all layers of the P0 cortex shows *mTOR* cKOs exhibit decreased soma size throughout S1 (II-IV: t_4=7.296, P=.001876; V: t_4=12.57, P=.000231; VI: t_4=9.835, P=.000599). Analyzed by multiple t-tests. N=3/genotype.

Results from *t*-tests indicated on graphs. Error bars represent mean +/- SEM. *P<.05, **P<.01, ***P<.001, ****P<.0001.

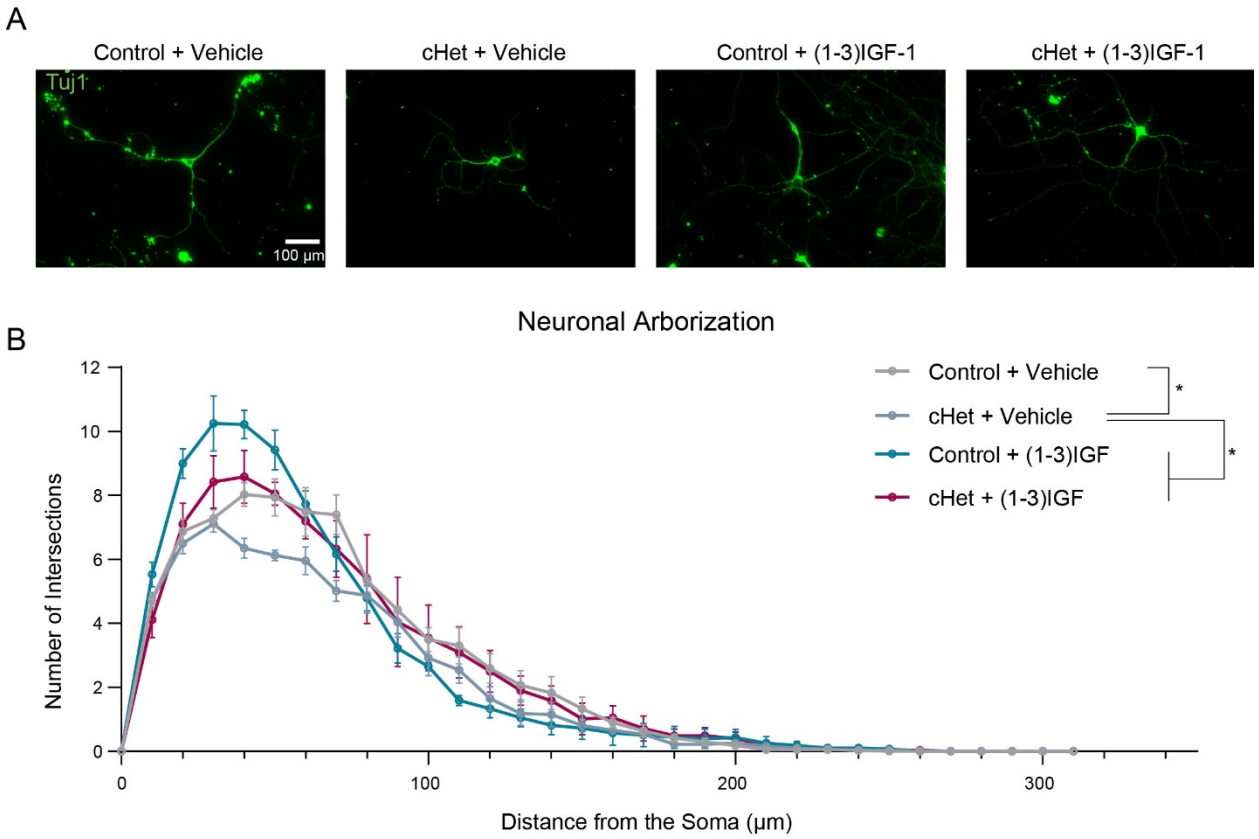

Supplemental Figure S8: Pharmacological treatment with (1-3)IGF-1 rescues decreased arborization of cHet neurons *in vitro*.

(A) Representative neurons at 40X magnification on DIV15 treated with vehicle or (1-3)IGF-1.

(B) Sholl analysis of neuronal arborization on individual neurons. Two-way ANOVA with Tukey's *post hoc* multiple comparisons tests on the area under the curve from the Sholl profile indicates a significant interaction between genotype and drug treatment ($F_{1,8}$=5.457, P=.0477), showing that cHet pyramidal neurons exhibit significantly decreased neuronal arborization. N=30-35 neurons from 3 animals/genotype/treatment group.

Results from *post hoc* tests indicated on graphs. Error bars represent mean +/- SEM. *P<.05, **P<.01, ***P<.001, ****P<.0001.

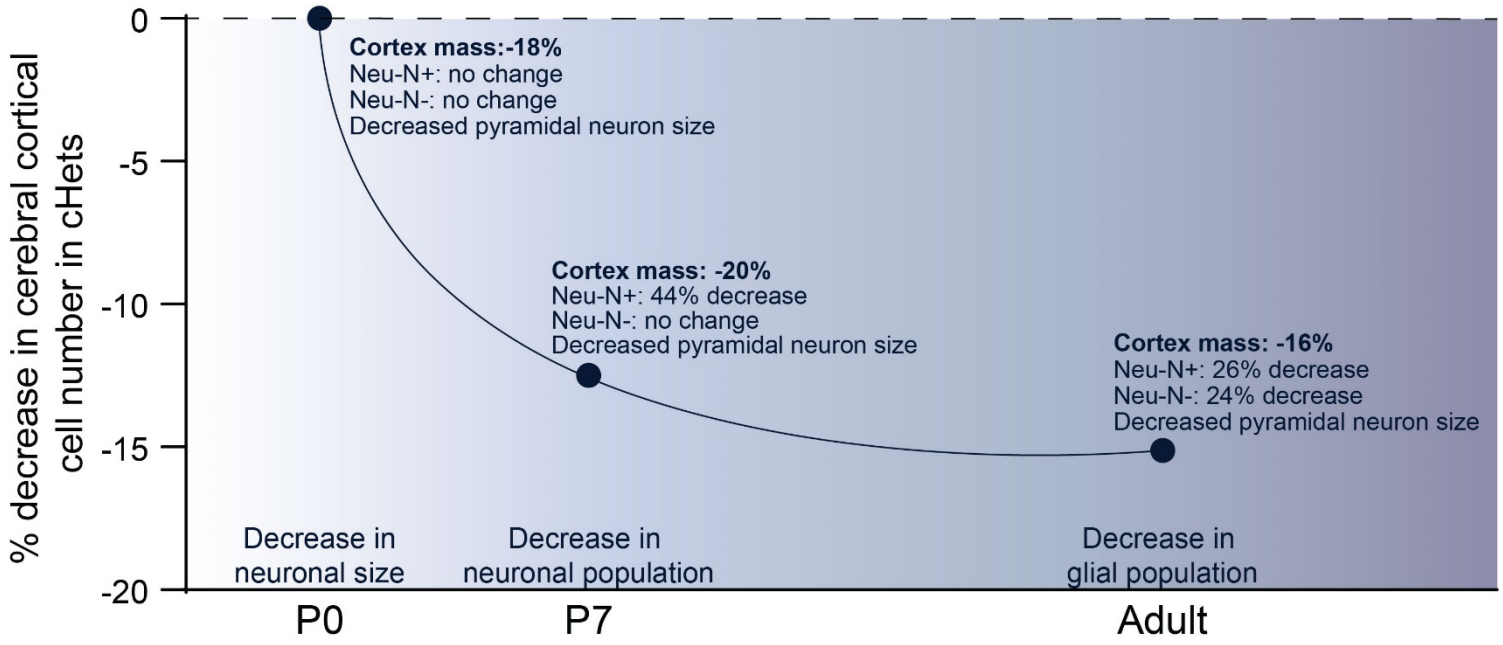

Supplemental Figure S9: Cellular events underlying altered postnatal brain growth trajectory in cHets.

At birth, decreased cortical mass in cHets is driven primarily by decreased neuronal size. Increased apoptosis between P0 and P7 causes a decrease in the cHet cortical cell number, which is driven by a decrease in the total neuronal population. Between P7 and adult, we hypothesize that non-neuronal cells are lost due to apoptosis, causing a more severe decrease in cell number driven by a reduction in both putative neuronal and glial populations. Note that this trajectory applies to *Dyrk1a* cHets, and the trajectory for other models, such as germline *Dyrk1a* mutants, may be somewhat different due to factors such as the timing of Cre-mediated recombination or the perdurance of Dyrk1a protein.

Supplementary Table S1: Significantly altered proteins in the cKO cortex at birth

Accession	Description	Abundance Ratio (log2): (*Dyrk1a* cKO) / (CTL)	Abundance Ratio Adj. P-Value: (*Dyrk1a* cKO) / (CTL)
Q8K0U4	Heat shock 70 kDa protein 12A OS=Mus musculus OX=10090 GN=Hspa12a PE=1 SV=1	-0.86	0.007016323
Q8BYI9	Tenascin-R OS=Mus musculus OX=10090 GN=Tnr PE=1 SV=2	-0.77	0.031120438
P35802	Neuronal membrane glycoprotein M6-a OS=Mus musculus OX=10090 GN=Gpm6a PE=1 SV=1	-0.76	0.002905811
Q8BHZ0	Protein FAM49A OS=Mus musculus OX=10090 GN=Fam49a PE=1 SV=1	-0.68	2.75E-05
Q62420	Endophilin-A1 OS=Mus musculus OX=10090 GN=Sh3gl2 PE=1 SV=2	-0.68	0.00090144
Q80ZF8	Adhesion G protein-coupled receptor B3 OS=Mus musculus OX=10090 GN=Adgrb3 PE=1 SV=2	-0.66	0.029438437
Q8CIQ7	Dedicator of cytokinesis protein 3 OS=Mus musculus OX=10090 GN=Dock3 PE=1 SV=1	-0.6	0.028900855
Q8BNA6	Protocadherin Fat 3 OS=Mus musculus OX=10090 GN=Fat3 PE=1 SV=2	-0.59	2.37E-05
Q80YX1	Tenascin OS=Mus musculus OX=10090 GN=Tnc PE=1 SV=1	-0.59	0.001238576
Q8JZK9	Hydroxymethylglutaryl-CoA synthase, cytoplasmic OS=Mus musculus OX=10090 GN=Hmgcs1 PE=1 SV=1	-0.58	2.37E-05
Q68FH0	Plakophilin-4 OS=Mus musculus GN=Pkp4	-0.56	1.40E-02
Q3ULJ0	Glycerol-3-phosphate dehydrogenase 1-like protein OS=Mus musculus OX=10090 GN=Gpd1l PE=1 SV=2	-0.55	0.000434322
Q62433	Protein NDRG1 OS=Mus musculus OX=10090 GN=Ndrg1 PE=1 SV=1	-0.55	0.014160484
Q8K0C4	Lanosterol 14-alpha demethylase OS=Mus musculus OX=10090 GN=Cyp51a1 PE=1 SV=1	-0.53	8.38E-05

Q8BHS8	Syntabulin OS=Mus musculus OX=10090 GN=Sybu PE=1 SV=1	-0.52	0.040969888
P31324	cAMP-dependent protein kinase type II-beta regulatory subunit OS=Mus musculus OX=10090 GN=Prkar2b PE=1 SV=3	-0.48	0.003814815
Q64521	Glycerol-3-phosphate dehydrogenase, mitochondrial OS=Mus musculus OX=10090 GN=Gpd2 PE=1 SV=2	-0.47	0.009404342
Q64487	Receptor-type tyrosine-protein phosphatase delta OS=Mus musculus OX=10090 GN=Ptprd PE=1 SV=3	-0.46	0.000192854
O35874	Neutral amino acid transporter A OS=Mus musculus OX=10090 GN=Slc1a4 PE=1 SV=1	-0.43	0.008296684
Q3UHD1	Adhesion G protein-coupled receptor B1 OS=Mus musculus OX=10090 GN=Adgrb1 PE=1 SV=1	-0.42	0.005558664
Q9EPN1	Neurobeachin OS=Mus musculus OX=10090 GN=Nbea PE=1 SV=1	-0.37	0.000813478
P62874	Guanine nucleotide-binding protein G(I)/G(S)/G(T) subunit beta-1 OS=Mus musculus OX=10090 GN=Gnb1 PE=1 SV=3	-0.37	0.029577302
P20357	Microtubule-associated protein 2 OS=Mus musculus OX=10090 GN=Map2 PE=1 SV=2	-0.36	0.010974796
Q7TPB0	Phospholipid phosphatase-related protein type 3 OS=Mus musculus OX=10090 GN=Plppr3 PE=1 SV=1	-0.35	0.03636148
Q9Z1B3	1-phosphatidylinositol 4,5-bisphosphate phosphodiesterase beta-1 OS=Mus musculus OX=10090 GN=Plcb1 PE=1 SV=2	-0.34	0.030604768
P97427	Dihydropyrimidinase-related protein 1 OS=Mus musculus OX=10090 GN=Crmp1 PE=1 SV=1	-0.33	0.007216898
Q2WF71	Leucine-rich repeat and fibronectin type III domain-containing protein 1 OS=Mus musculus OX=10090 GN=Lrfn1 PE=1 SV=1	-0.31	0.009404342
Q8R001	Microtubule-associated protein RP/EB family member 2 OS=Mus musculus OX=10090 GN=Mapre2 PE=1 SV=1	-0.31	0.02202471

Q8BXA0	Leucine-rich repeat and fibronectin type-III domain-containing protein 5 OS=Mus musculus GN=Lrfn5	-0.31	9.40E-03
P19096	Fatty acid synthase OS=Mus musculus OX=10090 GN=Fasn PE=1 SV=2	-0.29	2.37E-05
Q9EQF6	Dihydropyrimidinase-related protein 5 OS=Mus musculus OX=10090 GN=Dpysl5 PE=1 SV=1	-0.29	0.000349161
P70677	Caspase-3 OS=Mus musculus OX=10090 GN=Casp3 PE=1 SV=1	-0.29	0.010477032
P68369	Tubulin alpha-1A chain OS=Mus musculus OX=10090 GN=Tuba1a PE=1 SV=1	-0.28	0.000831939
P70207	Plexin-A2 OS=Mus musculus OX=10090 GN=Plxna2 PE=1 SV=2	-0.28	0.000831939
P83510	Traf2 and NCK-interacting protein kinase OS=Mus musculus OX=10090 GN=Tnik PE=1 SV=2	-0.28	0.007297581
P16546	Spectrin alpha chain, non-erythrocytic 1 OS=Mus musculus OX=10090 GN=Sptan1 PE=1 SV=4	-0.28	0.031120438
P70206	Plexin-A1 OS=Mus musculus OX=10090 GN=Plxna1 PE=1 SV=1	-0.28	0.047707398
P70206	Plexin-A1 OS=Mus musculus OX=10090 GN=Plxna1 PE=1 SV=1	-0.28	0.047707398
O08553	Dihydropyrimidinase-related protein 2 OS=Mus musculus OX=10090 GN=Dpysl2 PE=1 SV=2	-0.27	0.000396161
Q5SWU9	Acetyl-CoA carboxylase 1 OS=Mus musculus OX=10090 GN=Acaca PE=1 SV=1	-0.26	7.08E-08
P05214	Tubulin alpha-3 chain OS=Mus musculus GN=Tuba3a	-0.26	2.10E-03
P33173	Kinesin-like protein KIF1A OS=Mus musculus OX=10090 GN=Kif1a PE=1 SV=2	-0.24	0.002905811
O88844	Isocitrate dehydrogenase [NADP] cytoplasmic OS=Mus musculus OX=10090 GN=Idh1 PE=1 SV=2	-0.24	0.041965487
Q9JLB0	MAGUK p55 subfamily member 6 OS=Mus musculus OX=10090 GN=Mpp6 PE=1 SV=1	-0.23	0.000502933
Q7TMM9	Tubulin beta-2A chain OS=Mus musculus OX=10090 GN=Tubb2a PE=1 SV=1	-0.23	0.028887935

O88986	2-amino-3-ketobutyrate coenzyme A ligase, mitochondrial OS=Mus musculus OX=10090 GN=Gcat PE=1 SV=2	-0.22	0.020412475
P55821	Stathmin-2 OS=Mus musculus OX=10090 GN=Stmn2 PE=1 SV=1	-0.21	0.037922314
Q8K341	Alpha-tubulin N-acetyltransferase 1 OS=Mus musculus OX=10090 GN=Atat1 PE=1 SV=1	-0.2	0.012754859
Q91W69	Epsin-3 OS=Mus musculus OX=10090 GN=Epn3 PE=1 SV=1	-0.2	0.029448933
P35486	Pyruvate dehydrogenase E1 component subunit alpha, somatic form, mitochondrial OS=Mus musculus OX=10090 GN=Pdha1 PE=1 SV=1	-0.19	0.008489921
Q9D6R2	Isocitrate dehydrogenase [NAD] subunit alpha, mitochondrial OS=Mus musculus OX=10090 GN=Idh3a PE=1 SV=1	-0.18	0.004619461
P99024	Tubulin beta-5 chain OS=Mus musculus OX=10090 GN=Tubb5 PE=1 SV=1	-0.18	0.007016323
Q80XI4	Phosphatidylinositol 5-phosphate 4-kinase type-2 beta OS=Mus musculus OX=10090 GN=Pip4k2b PE=1 SV=1	-0.18	0.047707398
Q148V7	LisH domain and HEAT repeat-containing protein KIAA1468 OS=Mus musculus OX=10090 GN=Kiaa1468 PE=1 SV=1	-0.17	0.03636148
Q6IR34	G-protein-signaling modulator 1 OS=Mus musculus OX=10090 GN=Gpsm1 PE=1 SV=3	-0.11	0.042309357
P29341	Polyadenylate-binding protein 1 OS=Mus musculus OX=10090 GN=Pabpc1 PE=1 SV=2	0.15	0.037922314
P62962	Profilin-1 OS=Mus musculus OX=10090 GN=Pfn1 PE=1 SV=2	0.16	0.028887935
Q8BWT1	3-ketoacyl-CoA thiolase, mitochondrial OS=Mus musculus OX=10090 GN=Acaa2 PE=1 SV=3	0.16	0.040969888
Q99JY0	Trifunctional enzyme subunit beta, mitochondrial OS=Mus musculus OX=10090 GN=Hadhb PE=1 SV=1	0.18	0.01054324
P29758	Ornithine aminotransferase, mitochondrial OS=Mus musculus OX=10090 GN=Oat PE=1 SV=1	0.2	0.009404342

Q9DBJ1	Phosphoglycerate mutase 1 OS=Mus musculus OX=10090 GN=Pgam1 PE=1 SV=3	0.2	0.017565639
Q01853	Transitional endoplasmic reticulum ATPase OS=Mus musculus OX=10090 GN=Vcp PE=1 SV=4	0.2	0.043196596
P25444	40S ribosomal protein S2 OS=Mus musculus OX=10090 GN=Rps2 PE=1 SV=3	0.25	0.029577302
Q7TMK9	Heterogeneous nuclear ribonucleoprotein Q OS=Mus musculus OX=10090 GN=Syncrip PE=1 SV=2	0.25	0.047707398
Q9QX47	Protein SON OS=Mus musculus OX=10090 GN=Son PE=1 SV=2	0.26	0.032102808
P26039	Talin-1 OS=Mus musculus OX=10090 GN=Tln1 PE=1 SV=2	0.29	0.007297581
Q8BJW6	Eukaryotic translation initiation factor 2A OS=Mus musculus OX=10090 GN=Eif2a PE=1 SV=2	0.29	0.017289988
P26041	Moesin OS=Mus musculus OX=10090 GN=Msn PE=1 SV=3	0.32	0.025380268
Q8VEE4	Replication protein A 70 kDa DNA-binding subunit OS=Mus musculus OX=10090 GN=Rpa1 PE=1 SV=1	0.32	0.029577302
Q3TWW8	Serine/arginine-rich splicing factor 6 OS=Mus musculus OX=10090 GN=Srsf6 PE=1 SV=1	0.33	0.000813478
P51859	Hepatoma-derived growth factor OS=Mus musculus OX=10090 GN=Hdgf PE=1 SV=2	0.35	0.014160484
O35737	Heterogeneous nuclear ribonucleoprotein H OS=Mus musculus OX=10090 GN=Hnrnph1 PE=1 SV=3	0.35	0.043957411
P26043	Radixin OS=Mus musculus OX=10090 GN=Rdx PE=1 SV=3	0.36	0.006006015
P63276	40S ribosomal protein S17 OS=Mus musculus OX=10090 GN=Rps17 PE=1 SV=2	0.36	0.028900855
O88532	Zinc finger RNA-binding protein OS=Mus musculus OX=10090 GN=Zfr PE=1 SV=2	0.38	0.033566488
Q9QYB1	Chloride intracellular channel protein 4 OS=Mus musculus OX=10090 GN=Clic4 PE=1 SV=3	0.4	0.049950805

P28798	Granulins OS=Mus musculus OX=10090 GN=Grn PE=1 SV=2	0.41	0.005558664
Q61550	Double-strand-break repair protein rad21 homolog OS=Mus musculus OX=10090 GN=Rad21 PE=1 SV=3	0.45	0.03932378
Q8BT60	Copine-3 OS=Mus musculus OX=10090 GN=Cpne3 PE=1 SV=2	0.45	0.047024967
O35638	Cohesin subunit SA-2 OS=Mus musculus OX=10090 GN=Stag2 PE=1 SV=3	0.46	0.013631841
Q9D937	Uncharacterized protein C11orf98 homolog OS=Mus musculus OX=10090 PE=1 SV=1	0.48	0.02809097
Q99KC8	von Willebrand factor A domain-containing protein 5A OS=Mus musculus OX=10090 GN=Vwa5a PE=1 SV=2	0.48	0.029577302
P61025	Cyclin-dependent kinases regulatory subunit 1 OS=Mus musculus OX=10090 GN=Cks1b PE=3 SV=1	0.5	0.030304892
P48036	Annexin A5 OS=Mus musculus OX=10090 GN=Anxa5 PE=1 SV=1	0.51	0.00307869
P31786	Acyl-CoA-binding protein OS=Mus musculus OX=10090 GN=Dbi PE=1 SV=2	0.53	0.007016323
Q80ZV0	Ribonuclease H2 subunit B OS=Mus musculus OX=10090 GN=Rnaseh2b PE=1 SV=2	0.55	0.001238576
P16045	Galectin-1 OS=Mus musculus OX=10090 GN=Lgals1 PE=1 SV=3	0.58	0.014388696
P18242	Cathepsin D OS=Mus musculus OX=10090 GN=Ctsd PE=1 SV=1	0.92	2.37E-05
Q9DCJ9	N-acetylneuraminate lyase OS=Mus musculus OX=10090 GN=Npl PE=1 SV=1	1.06	0.036456158

Supplemental Table S2: Significantly altered phosphopeptides in the cKO cortex at birth.

Sequence	Modifications	Modifications (all possible sites)	Master Protein Accessions	Modifications in Master Proteins	Master Protein Descriptions	Protein Accessions	Abundance Ratio (log2): (*Dyrk1a* cKO) / (CTL)	Abundance Ratio Adj. P-Value: (*Dyrk1a* cKO) / (CTL)
ETEALLQSIGISPEPPLV PTPMSPSSK	1xOxidation [M22]; 1xTMT6plex [K27]; 1xTMT6plex [N-Term]; 2xPhospho [S12(100); S26(85.5)]	1xOxidation [M22]; 1xTMT6plex [K27]; 1xTMT6plex [N-Term]; 2xPhospho [T2(0); S8(0); S12(100); T20(1.6); S23(11.4); S25(1.6); S26(85.5)]	O88485	O88485 2xPhospho [S69(100); S83(85.5)]	Cytoplasmic dynein 1 intermediate chain 1 OS=Mus musculus OX=10090 GN=Dync1i1 PE=1 SV=2	O88485	-1.81	0.005979
ETEALLQSIGISPEPPLV PTPMSPSSK	1xTMT6plex [K27]; 1xTMT6plex [N-Term]; 2xPhospho [S12(100); S23(99.1)]	1xTMT6plex [K27]; 1xTMT6plex [N-Term]; 2xPhospho [T2(0); S8(0); S12(100); T20(0); S23(99.1); S25(0.9); S26(0)]	O88485	O88485 2xPhospho [S69(100); S80(99.1)]	Cytoplasmic dynein 1 intermediate chain 1 OS=Mus musculus OX=10090 GN=Dync1i1 PE=1 SV=2	O88485	-1.53	0.003061
ETEALLQSIGISPEPPLV PTPMSPSSK	1xTMT6plex [K27]; 1xTMT6plex [N-Term]; 1xPhospho [S/T]	1xTMT6plex [K27]; 1xTMT6plex [N-Term]; 1xPhospho [T2(0); S8(0);	O88485		Cytoplasmic dynein 1 intermediate chain 1 OS=Mus musculus	O88485	-1.52	0.004277

		S12(0); T20(0); S23(48.1); S25(3.7); S26(48.1)]			OX=10090 GN=Dync1i1 PE=1 SV=2			
ETEALLQSIGISPEPPLV PTPMSPSSK	1xOxidation [M22]; 1xTMT6plex [K27]; 1xTMT6plex [N-Term]; 1xPhospho [S26(90.8)]	1xOxidation [M22]; 1xTMT6plex [K27]; 1xTMT6plex [N-Term]; 1xPhospho [T2(0); S8(0); S12(0); T20(0); S23(0.8); S25(8.4); S26(90.8)]	O88485	O88485 1xPhospho [S83(90.8)]	Cytoplasmic dynein 1 intermediate chain 1 OS=Mus musculus OX=10090 GN=Dync1i1 PE=1 SV=2	O88485	-1.49	0.002371
HLSNVSSTGSIDMVDSP QLATLADEVSASLAK	1xDeamidated [N/Q]; 1xOxidation [M13]; 1xTMT6plex [K32]; 1xTMT6plex [N-Term]; 1xPhospho [S6(75.2)]	1xDeamidated [N4; Q18]; 1xOxidation [M13]; 1xTMT6plex [K32]; 1xTMT6plex [N-Term]; 1xPhospho [S3(11.2); S6(75.2); S7(11.2); T8(0.3); S10(1.8); S16(0.3); T21(0); S27(0); S29(0)]	P10637	P10637 1xPhospho [S704(75.2)]	Microtubule-associated protein tau OS=Mus musculus OX=10090 GN=Mapt PE=1 SV=3	sp; P10637	-1.21	0.026077

ETEALLQSIGISPEPPLVPTPMSPSSK	1xDeamidated [Q7]; 1xTMT6plex [K27]; 1xTMT6plex [N-Term]; 2xPhospho [S12(99.9); S23(84.1)]	1xDeamidated [Q7]; 1xTMT6plex [K27]; 1xTMT6plex [N-Term]; 2xPhospho [T2(0); S8(0.1); S12(99.9); T20(0.4); S23(84.1); S25(13.3); S26(2.2)]	O88485	O88485 2xPhospho [S69(99.9); S80(84.1)]	Cytoplasmic dynein 1 intermediate chain 1 OS=Mus musculus OX=10090 GN=Dync1i1 PE=1 SV=2	O88485	-1.11	0.009385
SAESLQSLNSGLCPEK	1xTMT6plex [K16]; 1xTMT6plex [N-Term]; 1xMMTS [C13]; 1xPhospho [S1(94.1)]	1xTMT6plex [K16]; 1xTMT6plex [N-Term]; 1xMMTS [C13]; 1xPhospho [S1(94.1); S4(5.9); S7(0); S10(0)]	Q3U5C7	Q3U5C7 1xPhospho [S592(94.1)]	Prickle-like protein 1 OS=Mus musculus OX=10090 GN=Prickle1 PE=1 SV=1	Q3U5C7	-0.88	0.013002
DLYQMSDSQLYEAFTFLK	1xTMT6plex [K18]; 1xTMT6plex [N-Term]	1xTMT6plex [K18]; 1xTMT6plex [N-Term]	P97427		Dihydropyrimidinase-related protein 1 OS=Mus musculus OX=10090 GN=Crmp1 PE=1 SV=1	P97427	-0.83	0.047553
QSQGTTPDTTPARTPTEEGTPTSEQNPFLFQEGK	1xTMT6plex [K34]; 1xTMT6plex [N-Term];	1xTMT6plex [K34]; 1xTMT6plex [N-Term];	Q8C8R3	Q8C8R3 2xPhospho [T3050(94.1); T/S]	Ankyrin-2 OS=Mus musculus OX=10090	Q8C8R3	-0.79	0.009385

	2xPhospho [T20(94.1); T/S]	2xPhospho [S2(0.1); T5(0.4); T6(12.1); T9(2.2); T10(2.2); T14(71.1); T16(12.2); T20(94.1); T22(2.9); S23(2.9)]			GN=Ank2 PE=1 SV=2			
QQESDDSLVDYGEGGE GQFNEDGSFIGQYTVK	1xTMT6plex [K32]; 1xTMT6plex [N-Term]; 1xPhospho [S/Y/T]	1xTMT6plex [K32]; 1xTMT6plex [N-Term]; 1xPhospho [S4(50); S7(50); Y11(0); S24(0); Y29(0); T30(0)]	Q810U3		Neurofascin OS=Mus musculus OX=10090 GN=Nfasc PE=1 SV=1	Q810U3	-0.76	0.047553
ASPVYLDILG	1xTMT6plex [N-Term]; 1xPhospho [Y5(94.8)]	1xTMT6plex [N-Term]; 1xPhospho [S2(5.2); Y5(94.8)]	P15209	P15209 1xPhospho [Y816(94.8)]	BDNF/NT-3 growth factors receptor OS=Mus musculus OX=10090 GN=Ntrk2 PE=1 SV=1	P15209	-0.74	0.006338
HLSNVSSTGSIDMVDSP QLATLADEVSASLAK	1xOxidation [M13]; 1xTMT6plex [K32]; 1xTMT6plex [N-Term];	1xOxidation [M13]; 1xTMT6plex [K32]; 1xTMT6plex [N-Term];	P10637	P10637 2xPhospho [S701(100); T706(79.3)]	Microtubule-associated protein tau OS=Mus musculus OX=10090	sp; P10637	-0.73	0.010918

	2xPhospho [S3(100); T8(79.3)]	2xPhospho [S3(100); S6(1.3); S7(9.7); T8(79.3); S10(9.7); S16(0); T21(0); S27(0); S29(0)]			GN=Mapt PE=1 SV=3			
DGSPDAPATPEKEEVAFSEYK	2xTMT6plex [K12; K21]; 1xTMT6plex [N-Term]; 1xPhospho [S3(100)]	2xTMT6plex [K12; K21]; 1xTMT6plex [N-Term]; 1xPhospho [S3(100); T9(0); S18(0); Y20(0)]	P20357	P20357 1xPhospho [S1352(100)]	Microtubule-associated protein 2 OS=Mus musculus OX=10090 GN=Map2 PE=1 SV=2	P20357	-0.73	0.02855
LAAGAESPQPASGNSPSEDDR	1xTMT6plex [N-Term]; 1xPhospho [S7(100)]	1xTMT6plex [N-Term]; 1xPhospho [S7(100); S12(0); S15(0); S17(0)]	P16054	P16054 1xPhospho [S329(100)]	Protein kinase C epsilon type OS=Mus musculus OX=10090 GN=Prkce PE=1 SV=1	P16054	-0.72	0.009385
TLYEEAEEASDISQQVANLAISPTTPGPSWPGDALR	1xTMT6plex [N-Term]; 1xPhospho [S22(85.9)]	1xTMT6plex [N-Term]; 1xPhospho [T1(0); Y3(0); S10(0); S13(0); S22(85.9); T24(12.3); T25(1.8); S29(0)]	Q9Z0E0	Q9Z0E0 1xPhospho [S448(85.9)]	Neurochondrin OS=Mus musculus OX=10090 GN=Ncdn PE=1 SV=1	Q9Z0E0	-0.71	0.047553

GVNFAEEPMRSDSENGEEEEAAEAGAFNAPVINR	1xTMT6plex [N-Term]; 1xPhospho [S]	1xTMT6plex [N-Term]; 1xPhospho [S11(50); S13(50)]	P31324		cAMP-dependent protein kinase type II-beta regulatory subunit OS=Mus musculus OX=10090 GN=Prkar2b PE=1 SV=3	P31324	-0.68	0.026077
EGTQASEGYFSQSQEEEFAQSEEPCAK	2xDeamidated [Q14; Q20]; 1xTMT6plex [K27]; 1xTMT6plex [N-Term]; 1xMMTS [C25]; 1xPhospho [S13(100)]	2xDeamidated [Q14; Q20]; 1xTMT6plex [K27]; 1xTMT6plex [N-Term]; 1xMMTS [C25]; 1xPhospho [T3(0); S6(0); Y9(0); S11(0); S13(100); S21(0)]	Q9QXS6	Q9QXS6 1xPhospho [S658(100)]	Drebrin OS=Mus musculus OX=10090 GN=Dbn1 PE=1 SV=4	Q9QXS6	-0.67	0.022482
HLSNVSSTGSIDMVDSPQLATLADEVSASLAK	1xOxidation [M13]; 1xTMT6plex [K32]; 1xTMT6plex [N-Term]; 1xPhospho [S/T]	1xOxidation [M13]; 1xTMT6plex [K32]; 1xTMT6plex [N-Term]; 1xPhospho [S3(5.7); S6(46.7); S7(46.7); T8(0.7); S10(0.1);	P10637		Microtubule-associated protein tau OS=Mus musculus OX=10090 GN=Mapt PE=1 SV=3	sp; P10637	-0.65	0.009385

		S16(0); T21(0); S27(0); S29(0)]						
DLYQMSDSQLYEAFTFLK	1xOxidation [M5]; 1xTMT6plex [K18]; 1xTMT6plex [N-Term]	1xOxidation [M5]; 1xTMT6plex [K18]; 1xTMT6plex [N-Term]	P97427		Dihydropyrimidinase-related protein 1 OS=Mus musculus OX=10090 GN=Crmp1 PE=1 SV=1	P97427	-0.63	0.047553
ASGQAFELILKPPSPISEAPR	1xDeamidated [Q4]; 1xTMT6plex [K11]; 1xTMT6plex [N-Term]; 1xPhospho [S17(98.9)]	1xDeamidated [Q4]; 1xTMT6plex [K11]; 1xTMT6plex [N-Term]; 1xPhospho [S2(0); S14(1.1); S17(98.9)]	P55821	P55821 1xPhospho [S65(98.9)]	Stathmin-2 OS=Mus musculus OX=10090 GN=Stmn2 PE=1 SV=1	P55821	-0.5	0.047553
LDDGHLNNSLGSPVQADVYFPR	1xTMT6plex [N-Term]; 1xPhospho [S12(100)]	1xTMT6plex [N-Term]; 1xPhospho [S9(0); S12(100); Y19(0)]	Q8VED9	Q8VED9 1xPhospho [S25(100)]	Galectin-related protein OS=Mus musculus OX=10090 GN=Lgalsl PE=1 SV=1	Q8VED9	-0.49	0.009385
NLASPEGTLATLGLK	1xTMT6plex [K15]; 1xTMT6plex [N-Term]; 1xPhospho [S4(100)]	1xTMT6plex [K15]; 1xTMT6plex [N-Term]; 1xPhospho	Q8BPN8	Q8BPN8 1xPhospho [S1856(100)]	DmX-like protein 2 OS=Mus musculus OX=10090	Q8BPN8	-0.48	0.021846

		[S4(100); T8(0); T11(0)]			GN=Dmxl2 PE=1 SV=3			
GVVESVVTIEDDFITVVQTTTDEGESGSHSVR	1xDeamidated [Q18]; 1xTMT6plex [N-Term]	1xDeamidated [Q18]; 1xTMT6plex [N-Term]	P20357		Microtubule-associated protein 2 OS=Mus musculus OX=10090 GN=Map2 PE=1 SV=2	P20357	-0.48	0.028687
SQGSPEDPPSQASPGSNK	1xTMT6plex [K18]; 1xTMT6plex [N-Term]; 1xPhospho [S13(98.1)]	1xTMT6plex [K18]; 1xTMT6plex [N-Term]; 1xPhospho [S1(0); S4(0); S10(0); S13(98.1); S16(1.9)]	Q6PGG2	Q6PGG2 1xPhospho [S247(98.1)]	GEM-interacting protein OS=Mus musculus OX=10090 GN=Gmip PE=1 SV=1	Q6PGG2	-0.47	0.016514
SQQQKPEEEAVSSSQSPTATEIPGPLGSGLMPPLPFFNK	1xOxidation [M31]; 2xTMT6plex [K5; K39]; 1xTMT6plex [N-Term]; 1xPhospho [S/T]	1xOxidation [M31]; 2xTMT6plex [K5; K39]; 1xTMT6plex [N-Term]; 1xPhospho [S1(0.5); S12(36.1); S13(36.1); S14(8.4); S16(8.4); T18(8.4); T20(2.1); S28(0)]	Q8K0T0		Reticulon-1 OS=Mus musculus OX=10090 GN=Rtn1 PE=1 SV=1	Q8K0T0	-0.47	0.047553
HLSNVSSTGSIDMVDSPQLATLADEVSASLAK	1xTMT6plex [K32];	1xTMT6plex [K32];	P10637		Microtubule-associated	sp; P10637	-0.46	0.025633

	1xTMT6plex [N-Term]; 1xPhospho [S/T]	1xTMT6plex [N-Term]; 1xPhospho [S3(5.8); S6(46.7); S7(46.7); T8(0.8); S10(0.1); S16(0); T21(0); S27(0); S29(0)]			protein tau OS=Mus musculus OX=10090 GN=Mapt PE=1 SV=3			
VYNDGEQIIAQGDLADS FFIVESGEVK	1xTMT6plex [K27]; 1xTMT6plex [N-Term]	1xTMT6plex [K27]; 1xTMT6plex [N-Term]	P31324		cAMP-dependent protein kinase type II-beta regulatory subunit OS=Mus musculus OX=10090 GN=Prkar2b PE=1 SV=3	P31324	-0.45	0.025633
ASQPSPPAQEAGYSTL AQSYTPDHPSELPEEP SSPQER	1xTMT6plex [N-Term]; 1xPhospho [S/Y/T]	1xTMT6plex [N-Term]; 1xPhospho [S2(0); S5(0); Y13(0); S14(0); T15(0); S19(0); Y20(0); T21(0); S26(0); S33(50); S34(50)]	P20357		Microtubule-associated protein 2 OS=Mus musculus OX=10090 GN=Map2 PE=1 SV=2	P20357	-0.44	0.009385

SKESVPDFPLSPPKK	3xTMT6plex [K2; K14; K15]; 1xTMT6plex [N-Term]; 1xPhospho [S11(100)]	3xTMT6plex [K2; K14; K15]; 1xTMT6plex [N-Term]; 1xPhospho [S1(0); S4(0); S11(100)]	P54227	P54227 1xPhospho [S38(100)]	Stathmin OS=Mus musculus OX=10090 GN=Stmn1 PE=1 SV=2	P54227	-0.44	0.014405
NFLNALTSPIEYQR	1xTMT6plex [N-Term]; 1xPhospho [S8(99.9)]	1xTMT6plex [N-Term]; 1xPhospho [T7(0.2); S8(99.9); Y12(0)]	Q0KL02	Q0KL02 1xPhospho [S2282(99.9)]	Triple functional domain protein OS=Mus musculus OX=10090 GN=Trio PE=1 SV=3	Q0KL02	-0.42	0.016514
EQPGNTVSSGQEDFPS VLFETAASLPSLSPLST VSFK	1xTMT6plex [K37]; 1xTMT6plex [N-Term]; 1xPhospho [S29(98)]	1xTMT6plex [K37]; 1xTMT6plex [N-Term]; 1xPhospho [T6(0); S8(0); S9(0); S16(0); T21(0); S24(0); S27(1.7); S29(98); S32(0.2); T33(0); S35(0)]	Q99P72	Q99P72 1xPhospho [S223(98)]	Reticulon-4 OS=Mus musculus OX=10090 GN=Rtn4 PE=1 SV=2	Q99P72	-0.42	0.047553
HLSNVSSTGSIDMVDSP QLATLADEVSASLAK	1xTMT6plex [K32]; 1xTMT6plex [N-Term]; 2xPhospho	1xTMT6plex [K32]; 1xTMT6plex [N-Term]; 2xPhospho	P10637	P10637 2xPhospho [S705(81.8); T706(83.4)]	Microtubule-associated protein tau OS=Mus musculus	sp; P10637	-0.41	0.026041

	[S7(81.8); T8(83.4)]	[S3(3.1); S6(15.8); S7(81.8); T8(83.4); S10(15.8); S16(0); T21(0); S27(0); S29(0)]			OX=10090 GN=Mapt PE=1 SV=3			
RPVSVSPSSSQEISENQYAVICSEK	1xDeamidated [Q17]; 1xTMT6plex [K25]; 1xTMT6plex [N-Term]; 1xMMTS [C22]; 1xPhospho [S/Y]	1xDeamidated [Q17]; 1xTMT6plex [K25]; 1xTMT6plex [N-Term]; 1xMMTS [C22]; 1xPhospho [S4(0); S6(0.1); S8(46.7); S9(46.7); S10(6.3); S14(0.1); Y18(0); S23(0)]	Q8K400		Syntaxin-binding protein 5 OS=Mus musculus OX=10090 GN=Stxbp5 PE=1 SV=3	Q8K400	-0.37	0.049214
MDSYEQEEDIDQIVAEVK	1xOxidation [M1]; 1xTMT6plex [K18]; 1xTMT6plex [N-Term]; 1xPhospho [S/Y]	1xOxidation [M1]; 1xTMT6plex [K18]; 1xTMT6plex [N-Term]; 1xPhospho [S3(50); Y4(50)]	B2RUJ5		Amyloid-beta A4 precursor protein-binding family A member 1 OS=Mus musculus OX=10090 GN=Apba1 PE=1 SV=2	B2RUJ5	-0.36	0.035409

DGEPIENEEEDDEKHIFSDDSSELTIR	1xTMT6plex [K14]; 1xTMT6plex [N-Term]	1xTMT6plex [K14]; 1xTMT6plex [N-Term]	P13595		Neural cell adhesion molecule 1 OS=Mus musculus OX=10090 GN=Ncam1 PE=1 SV=3	P13595	-0.33	0.037376
ALYLEPSDGVSPTQETGEAQSQDDER	1xTMT6plex [N-Term]; 1xPhospho [S11(97.2)]	1xTMT6plex [N-Term]; 1xPhospho [Y3(0); S7(1.4); S11(97.2); T13(1.4); T16(0); S21(0)]	Q6ZPE2	Q6ZPE2 1xPhospho [S706(97.2)]	Myotubularin-related protein 5 OS=Mus musculus OX=10090 GN=Sbf1 PE=1 SV=2	Q6ZPE2	-0.3	0.009385
APPASKASPAPTPTPAGAASPLAAVAAPATDAPQAK	2xTMT6plex [K6; K36]; 1xTMT6plex [N-Term]; 1xPhospho [S5(81.4)]	2xTMT6plex [K6; K36]; 1xTMT6plex [N-Term]; 1xPhospho [S5(81.4); S8(7.6); T12(7.6); T14(2.5); S20(0.9); T30(0)]	P13595	P13595 1xPhospho [S943(81.4)]	Neural cell adhesion molecule 1 OS=Mus musculus OX=10090 GN=Ncam1 PE=1 SV=3	P13595	-0.25	0.047226
KEGGGDSSASSPTEEEQEQGEMSACSDEGTAQEGK	1xOxidation [M22]; 2xTMT6plex [K1; K35]; 1xTMT6plex [N-Term]; 1xMMTS [C25];	1xOxidation [M22]; 2xTMT6plex [K1; K35]; 1xTMT6plex [N-Term]; 1xMMTS [C25];	P28667	P28667 1xPhospho [S135(99.8)]	MARCKS-related protein OS=Mus musculus OX=10090 GN=Marcksl1 PE=1 SV=2	P28667	-0.2	0.025633

	1xPhospho [S26(99.8)]	1xPhospho [S7(0); S8(0); S10(0); S11(0); T13(0); S23(0.2); S26(99.8); T30(0)]						
AQSGSPESSSGQTK	1xTMT6plex [K14]; 1xTMT6plex [N-Term]; 1xPhospho [S3(92.9)]	1xTMT6plex [K14]; 1xTMT6plex [N-Term]; 1xPhospho [S3(92.9); S5(7.1); S8(0); S9(0); S10(0); T13(0)]	Q8BXJ2	Q8BXJ2 1xPhospho [S488(92.9)]	Transcriptional-regulating factor 1 OS=Mus musculus OX=10090 GN=Trerf1 PE=1 SV=1	Q8BXJ2	0.22	0.009385
YLQDDTSDPTYTSSLGGK	1xTMT6plex [K18]; 1xTMT6plex [N-Term]; 1xPhospho [T6(87.8)]	1xTMT6plex [K18]; 1xTMT6plex [N-Term]; 1xPhospho [Y1(1.4); T6(87.8); S7(10.7); T10(0); Y11(0); T12(0); S13(0); S14(0)]	Q8CBF3	Q8CBF3 1xPhospho [T773(87.8)]	Ephrin type-B receptor 1 OS=Mus musculus OX=10090 GN=Ephb1 PE=1 SV=1	Q8CBF3	0.24	0.047553
SISEGHPWHVPDSPSHSK	1xTMT6plex [K18]; 1xTMT6plex [N-Term]; 1xPhospho [S13(82.4)]	1xTMT6plex [K18]; 1xTMT6plex [N-Term]; 1xPhospho [S1(0); S3(0);	Q6ZWQ0	Q6ZWQ0 1xPhospho [S6448(82.4)]	Nesprin-2 OS=Mus musculus OX=10090 GN=Syne2 PE=1 SV=2	Q6ZWQ0	0.45	0.002476

		S13(82.4); S15(2.9); S17(14.7)]						
RWTDLLSK	1xTMT6plex [K8]; 1xTMT6plex [N-Term]; 1xPhospho [T3(100)]	1xTMT6plex [K8]; 1xTMT6plex [N-Term]; 1xPhospho [T3(100); S7(0)]	Q9QXZ0	Q9QXZ0 1xPhospho [T5394(100)]	Microtubule-actin cross-linking factor 1 OS=Mus musculus OX=10090 GN=Macf1 PE=1 SV=2	Q9QXZ0	0.48	0.01183
QTPPASPSPQPIEDRPPSSPIYEDAAPFK	1xTMT6plex [K29]; 1xTMT6plex [N-Term]; 1xPhospho [S/Y/T]	1xTMT6plex [K29]; 1xTMT6plex [N-Term]; 1xPhospho [T2(0); S6(0); S8(0); S18(33.3); S19(33.3); Y22(33.3)]	Q60598		Src substrate cortactin OS=Mus musculus OX=10090 GN=Cttn PE=1 SV=2	Q60598	0.54	0.047553
DQGSCGSCWAFGAVEAISDR	1xTMT6plex [N-Term]; 2xMMTS [C5; C8]	1xTMT6plex [N-Term]; 2xMMTS [C5; C8]	P10605		Cathepsin B OS=Mus musculus OX=10090 GN=Ctsb PE=1 SV=2	P10605	0.65	0.034944
TVDLQDAEEAVELVQYAYFK	1xDeamidated [Q5]; 1xTMT6plex [K20]; 1xTMT6plex [N-Term]	1xDeamidated [Q5]; 1xTMT6plex [K20]; 1xTMT6plex [N-Term]	P25206		DNA replication licensing factor MCM3 OS=Mus musculus OX=10090 GN=Mcm3 PE=1 SV=2	P25206	0.82	0.047553

AVESTDEDHQTDLDAK	1xTMT6plex [K16]; 1xTMT6plex [N-Term]; 1xPhospho [S4(93.9)]	1xTMT6plex [K16]; 1xTMT6plex [N-Term]; 1xPhospho [S4(93.9); T5(6.1); T11(0)]	Q8BLH7	Q8BLH7 1xPhospho [S134(93.9)]	HIRA-interacting protein 3 OS=Mus musculus OX=10090 GN=Hirip3 PE=1 SV=1	Q8BLH7	0.84	0.015071
AADEDWDSELEDDLLGEDLLSGK	1xTMT6plex [K23]; 1xTMT6plex [N-Term]; 1xPhospho [S8(100)]	1xTMT6plex [K23]; 1xTMT6plex [N-Term]; 1xPhospho [S8(100); S21(0)]	Q9CXK9	Q9CXK9 1xPhospho [S41(100)]	RNA-binding protein 33 OS=Mus musculus OX=10090 GN=Rbm33 PE=1 SV=2	Q9CXK9	0.84	0.03619
KASEDESDLEDEEEKSQEDTEQK	3xTMT6plex [K1; K15; K23]; 1xTMT6plex [N-Term]; 1xPhospho [S7(99.7)]	3xTMT6plex [K1; K15; K23]; 1xTMT6plex [N-Term]; 1xPhospho [S3(0.3); S7(99.7); S16(0); T20(0)]	P25206	P25206 1xPhospho [S672(99.7)]	DNA replication licensing factor MCM3 OS=Mus musculus OX=10090 GN=Mcm3 PE=1 SV=2	P25206	0.92	0.024414
TPLATIADQQQLQLSPLKR	1xDeamidated [Q11]; 1xTMT6plex [K18]; 1xTMT6plex [N-Term]; 1xPhospho [S15(100)]	1xDeamidated [Q11]; 1xTMT6plex [K18]; 1xTMT6plex [N-Term]; 1xPhospho [T1(0); T5(0); S15(100)]	P11157	P11157 1xPhospho [S20(100)]	Ribonucleoside-diphosphate reductase subunit M2 OS=Mus musculus OX=10090 GN=Rrm2 PE=1 SV=1	P11157	1.17	0.015071
LVGSGFPLPTSDLDDSLTEDIDEK	1xTMT6plex [K24];	1xTMT6plex [K24];	Q91YU3	Q91YU3 2xPhospho	Myb/SANT-like DNA-	Q91YU3	1.21	0.014405

	1xTMT6plex [N-Term]; 2xPhospho [S11(89.7); S16(89.7)]	1xTMT6plex [N-Term]; 2xPhospho [S4(0); T10(10.3); S11(89.7); S16(89.7); T18(10.3)]		[S101(89.7); S106(89.7)]	binding domain-containing protein 4 OS=Mus musculus OX=10090 GN=Msantd4 PE=2 SV=1			
IGEGTYGVVYK	1xTMT6plex [K11]; 1xTMT6plex [N-Term]; 2xPhospho [T5(100); Y6(100)]	1xTMT6plex [K11]; 1xTMT6plex [N-Term]; 2xPhospho [T5(100); Y6(100); Y10(0)]	P11440	P11440 2xPhospho [T14(100); Y15(100)]	Cyclin-dependent kinase 1 OS=Mus musculus OX=10090 GN=Cdk1 PE=1 SV=3	P97377; P11440; Q80YP0	1.56	0.029806